Journal of the Korean Nuclear Society
Volume 27, Number 5, October 1995

The LQG/LTR Dynamic Digital Control System Design for the Nuclear Steam Generator Water Level

Yoon Joon Lee
Cheju National University
(Received March 27, 1995)

증기발생기 디지탈 수위조절 시스템의 LQG / LTR 동적 제어설계

이윤준
제주대학교
(1995. 3. 27 접수)

Abstract

The steam generator feedwater and level control system is designed by two steps of the feedwater control design and the feedback loop controller design. The feedwater servo system is designed by the optimal LQR/LQG approach and then is modified by the LTR method to recover the robustness. The plant characteristics are subject to change with the power variation and these dynamic properties are considered in the design of the feedback controller. All the designs are made in the continuous domain and are digitalized by applying the proper sampling period. The system is simulated for the two cases of power increase and decrease. From the results of simulation, it is found that the controller constants would rather be invariable during the power increase, while for the case of power decrease they should be changed with the power variation to keep the system stability.

요 약

증기발생기의 급수 및 수위조절 시스템과 관련하여 전체 시스템을 급수 서보시스템과 궤환제어기로 나누어 설계하였다. 급수 시스템의 설계에는 최적제어이론을 사용하였으며 시스템의 강인성을 위하여 다시 LTR 기법을 이용하였다. 증기발생기의 제어특성은 열수력학적인 이유에 의하여 출력에 따라 계속적으로 변하게 되므로 궤환제어기가 이러한 변화를 동적으로 반영할 수 있도록 하였다. 모든 설계는 연속시스템에서 이루어졌으며 적절한 샘플링 주기를 선정하여 디지탈화 하였다. 이같은 시스템을 이용하여 출력증가 및 감소의 두가지에 대해 검토한 결과, 출력의 증가시에는 제어상수를 고정시키는 것이 바람직하나 출력의 감소시에는 시스템의 안정을 위하여 제어상수가 출력에 따라 동적으로 변화해야 함을 알 수 있었다.

1. Introduction

The steam generator is one of important equipments in the nuclear power plant. It functions as a boundary between the primary and the secondary systems. It is a heat source to the secondary system and at the time, it is a heat sink of the primary system. Therefore the steam generator should maintain the sufficient amount of water. However too much water raises the problem of moisture carry-over to the steam turbine, which is critical to the turbine life. Because of these problems, limitations are imposed both on the upper and lower bounds of water level. But it is very difficult to maintain the steam generator water level within the permissible span when the power is low. Particularly during the start up, a great attention should be paid by an operator, and the trip occurred by breaching the level limitations is one of main causes of lowering the plant availability. Presently several systems [1], [2] are developed and installed to control the level automatically and show a good performance. They are still PID based ones, while a number of important issues concerning the controller design, robustness, integrity and stability have been addressed by modern control theory.

In the light of control, the steam generator feedwater and level control system is a kind of regulating system. The steam flow rate and other feedbacked signals generate a driving signal which controls the feedwater flow rate to keep the level constant, and at the same time it includes the servo system which is to match the feedwater flow rate to the steam flow rate. The steam flow rate is not only a command signal to the system but also is a disturbance to the steam generator. In designing the feedwater control system, two points are to be considered. One is the uncertainty of plant and measurement, and the other is the limitation on the feedwater valve motion. To reflect these problems together on design, the optimal design of the LQR/LQG is preferable to the existing classical design. However, the optimal design stresses too much the minimization of the performance index, or cost function, and may raise the problem of robustness. Therefore, the loop transfer recovery (LTR) method is used in this study to guarantee the performance robustness.

In should be noted that the thermal-hydraulic properties of the steam generator are subject to change with the power variations. As is well known, the feedback gain should be decreased to maintain the stability at low power, while it can be increased to boost the system speed in high power ranges. In the previous studies [3], [4], [5], the plant properties were described in terms of the power at which the transient starts and were assumed to be constant until the system reaches a new steady state. But in reality, all the plant characteristics change with the power variations, and these dynamic properties are taken into account in this study. All the designs are made in the continuous domain and the controller determined in the continuous domain is converted to the digital controller. Sufficient consideration is given to the selection of the sampling period, which is a critical issue in digital control design.

The contents of this paper are outlined as below. First, the feedwater control system is designed with the LQG/LTR method and its robustness is discussed. Then the plant properties are defined in terms of power to investigate the dynamic control parameters. Finally, the digitalization of the controller is discussed together with the results of numerical simulations.

2. LQG/LTR Design of Feedwater Control System

The steam generator feedwater and level control system is described in Fig. 1. It employs three elements of steam flow rate, feedwater flow rate and steam generator water level. The feedwater flow rate and the level signals are feedbacked, and are summed with the input signal of steam flow rate to generate a feedwater control signal. In addition, the steam flow rate, primary coolant temperature and feedwater temperature act on the steam generator as

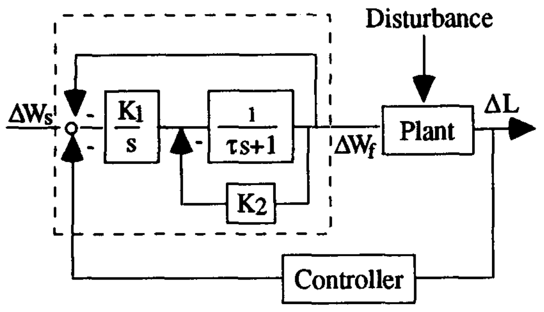

Fig. 1. Steam Generator Level and Feedwater Control System

disturbance signals. As shown in the figure, the overall control system design can be divided into two steps, that is, the design of the feedwater station and the determination of the controller located on the feedback loop.

The feedwater control system, dotted part of Fig. 1, is a servo system of which the output of feedwater flow rate should follow the input of steam flow rate. The open loop valve dynamics is approximated as a first order lagger whose time constant is τ, and can be written in the first order state variables.

$$\dot{x} = ax + bu, \quad y = cx + du \tag{1}$$

Since the feedwater station is a servo system, it is a common practice to introduce an integrator to eliminate the steady state errors. By defining the integrator gain as K_1 and the feedback gain as K_2, the feedwater servo system can be converted to the regulation system by variable transformation as follows.

$$\dot{\xi} = \mathbf{A}\xi + \mathbf{B}w, \quad \varsigma = \mathbf{C}\xi + \mathbf{D}w$$

$$w = -\mathbf{K}\xi$$

where

$$\mathbf{A} = \begin{bmatrix} a & b \\ 0 & 0 \end{bmatrix}, \ \mathbf{B} = \begin{bmatrix} 0 \\ b \end{bmatrix}, \ \mathbf{C} = [c \quad 0], \text{ and } \mathbf{D} = [0]. \tag{2}$$

Equation (2) is a regulating system and the optimal feedback gain can be determined by the LQR (Linear Quadratic Regulating) method. With the state and input weighting matrices of $\mathbf{Q}$ and $\mathbf{R}$, the ARE (Algebraic Riccati Equation) is

$$\mathbf{A}^T\mathbf{P} + \mathbf{P}\mathbf{A} + \mathbf{Q} - \mathbf{P}\mathbf{B}\mathbf{R}^{-1}\mathbf{B}^T\mathbf{P} = \mathbf{0} \tag{3}$$
$$\mathbf{Q} = q\cdot[\mathbf{C}^T\mathbf{C}], \quad \mathbf{R} = r\cdot\mathbf{I}$$

Then the optimal gains of K_1 and K_2 are determined as

$$\mathbf{K} = \mathbf{R}^{-1}\mathbf{B}^T\mathbf{P} = [K_1c - K_2a \quad -K_2b] \tag{4}$$

The ratio of two weighting matrices has a strong influence on the system characteristics. For example, as r increases, a greater penalty is imposed on the input energy and the system becomes more stable, but at the expense of slower speed. With the valve time constant of 1 sec, numerous values of q/r is checked with respect to various control specifications and traded off as $q = r = 1$. The gains are $\mathbf{K} = [0.2679 \quad 0.7321]$, or $[K_1 \ K_2] = [1.0 \quad 0.7321]$, and the system poles are located at $[-0.8660 \pm j0.5]$. The frequency responses show that the system has a sufficient phase margin of 81 degrees, which is the benefit of the LQR design.

It is well known that the feedwater measurement has a great uncertainty, particularly at the low power levels, and the noised signal is not proper to be feedbacked. In this situation, it is desirable to build an optimal observer by the LQG (Linear Quadratic Gaussian) method to estimate the feedwater signal. But it is necessary to consider the robustness of the compensator designed by the LQG approach. The issue is that in any actual situation the plant dynamics may not be exactly known, and there may exist disturbances in the system. The compensator should provide not only good performance but also performance robustness in the face of disturbances and stability robustness in the presence of unmodeled plant dynamics.

In general, the LQG dynamic regulator has no guaranteed robustness [6], in contrast with the LQR regulator which guarantees the robustness with infinite gain margin and more than 60 degrees phase margin. Other problems with the LQG is that it requires statistical information of the noise process, which is either unavailable or is impractical to obtain in most cases. However, the robustness of the LQR hints that by selecting the design parameters of observer weighting matrices, the LQG can approximately recover the LQR properties. The LQR system is given by

$$M(s) = \mathbf{K}(s\mathbf{I} - \mathbf{A})^{-1}\mathbf{B} = \mathbf{K}\mathbf{\Phi}\mathbf{B} \quad (5)$$

where $\mathbf{K}$ is the feedback gain obtained from Eq.(4), and $\mathbf{\Phi}$ is the resolvent matrix.

Equation (5) is the target feed loop (TFL) of the LTR (Loop Transfer Recovery), and the selection of noise variance matrices of the LQG is made in such a way that the resulting closed loop system can be approached to the TFL as far as possible. For the system with measurement and system noised the loop transfer function of the LQG is

$$\begin{aligned} M(s)_{LQG} &= \mathbf{K}(s\mathbf{I} - \mathbf{A} + \mathbf{B}\mathbf{K} + \mathbf{L}\mathbf{C})^{-1}\mathbf{L}\mathbf{C}(s\mathbf{I} - \mathbf{A})^{-1}\mathbf{B} \\ &= \mathbf{K}\mathbf{\Phi}_r(s)\mathbf{L}\mathbf{C}\mathbf{\Phi}_0(s)\mathbf{B} \end{aligned} \quad (6)$$

Under the conditions of that the plant, $\mathbf{C}\mathbf{\Phi}_0(s)\mathbf{B}$, is non-minimum, and $E(\mathbf{v}\mathbf{v}^T) = \mathbf{R}_0 = \mathbf{I}$, $E(\mathbf{w}\mathbf{w}^T) = \mathbf{Q}_0 = q^2\mathbf{B}\mathbf{B}^T$, the following relationship can be derived by the matrix inversion lemma [7].

$$\lim_{q \to \infty} M(s)_{LQG} = M(s)_{LQR} \quad (7)$$

Then by controlling the process noise spectral density $\mathbf{Q}_0$, which is a key parameter of the LQG design, the optimal observer gain is obtained by solving the filter Riccati equation below.

$$\mathbf{A}\mathbf{P} + \mathbf{P}\mathbf{A}^T + q^2\mathbf{B}\mathbf{B}^T - \mathbf{P}\mathbf{C}^T\mathbf{C}\mathbf{P} = \mathbf{0}, \quad \mathbf{L} = \mathbf{P}\mathbf{C}^T \quad (8)$$

Figure 2 is the Bode diagram of the system for various values of $\mathbf{Q}_0$, and the corresponding system step responses are described in Fig. 3.

As q or $\mathbf{Q}_0$ increases, the LQR target feed loop is recovered. From these results, q is determined as 150 and the observer gain is $\mathbf{L} = [16.35 \quad 150]$. The phase margin is about 77 degrees and the observer

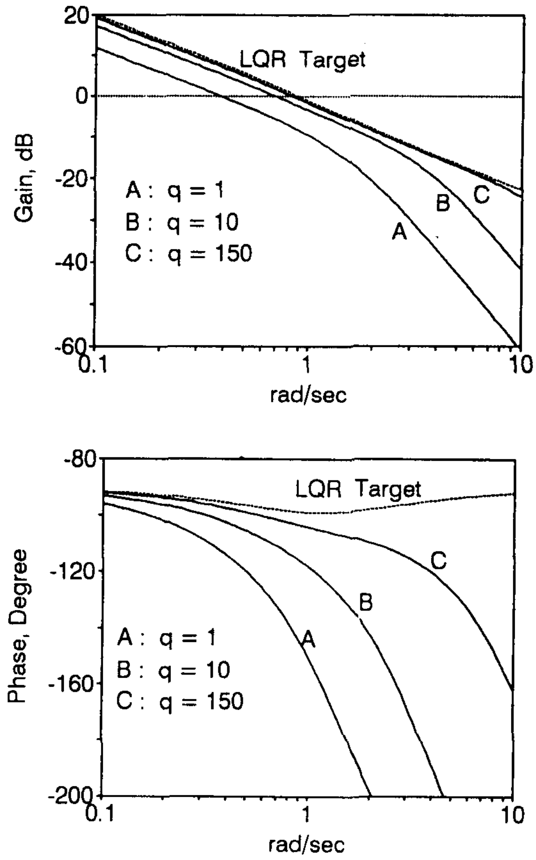

Fig. 2. Bode Diagram of LTR for Various Weights

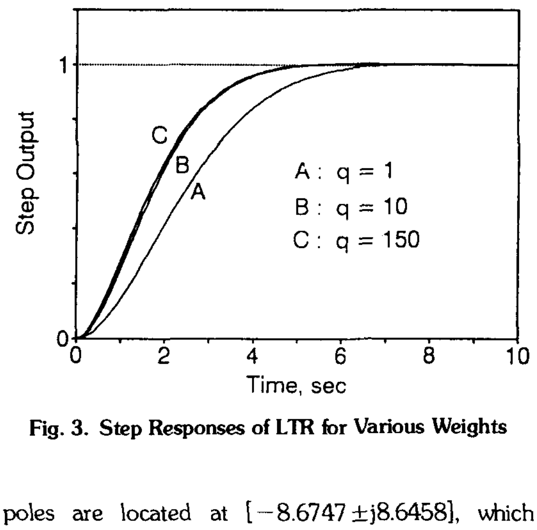

Fig. 3. Step Responses of LTR for Various Weights

poles are located at $[-8.6747 \pm j8.6458]$, which shows a faster speed than that of the system. The feedwater controller designed so far, in the form of transfer function, is

$$H(s) = \frac{114.1884\,s + 150}{s^2 + 18.0814\,s + 162.9686} \qquad (9)$$

The system properties become different depending on the location of the controller. In the parallel configuration, the controller is located on the feedback loop and in the cascaded configuration, the controller is in series with the plant with the unity feedback. In general, the cascaded configuration is better than the parallel one with respect to the tracking capability and robustness to the system noise. Hence the feedwater controller is determined to be located in series with the plant, as described in Fig. 4.

To investigate the robustness of the feedwater system designed above, a plant disturbance is considered. Suppose that the ideal plant and perturbed plant be $\mathbf{R}(s)$ and $\tilde{\mathbf{R}}(s)$ respectively, then

$$R(s) = G(s)K(s),\ \ \tilde{R}(s) = R(s)D(s) \qquad (10)$$

where D(s) is a disturbance function. As a disturbance function of D(s), a delay function is used in this study. The reasons of using the delay as a disturbance function are that there is a mechanical delay in torque transfer, and that this type of disturbance sustains for a long period. Since the effect of perturbation continues for a long time, it is a severer disturbance than the diminishing oscillatory disturbances. The delay function can be put into as

$$D(s) = 1 - s\tau + \frac{1}{2!}(s\tau)^2 + \frac{1}{3!}(s\tau)^3 \cdots \cong 1 - s\tau + \frac{1}{2!}(s\tau)^2 \qquad (11)$$

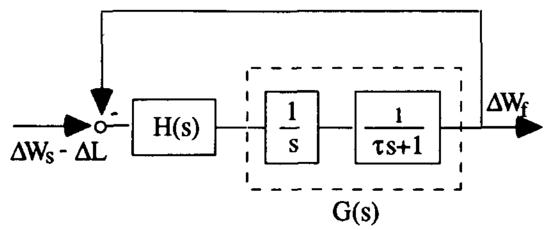

Fig. 4. Configuration of Feedwater Controller

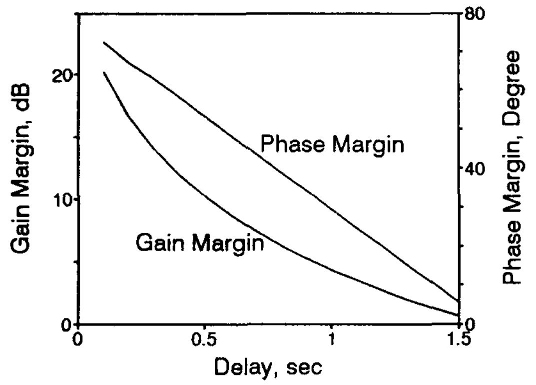

Fig. 5. System Margins by Delay Time

Figure 5 shows both the gain margins and phase margins of the feedwater system for various magnitudes of delay time. It can be known that the feedwater system designed by the LTR approach is stable in face of the disturbance whose delay is about up to 1.5 times the time constant of the original plant. Further, since the disturbance is approximated to the second order system, Eq.(11) is severer than the actual disturbance and the actual margin would be greater with the larger delays than those shown in the figure.

The robustness of the system can also be verified by modeling the uncertainty. The additive and multiplicative uncertainty models are defined as below [8].

$$\Delta a(s) = \tilde{R}(s) - R(s),\ \ \Delta m(s) = \Delta a(s)/R(s) \qquad (12)$$

The sensitivity (S), complementary sensitivity (T) and the inverse difference (J) of the system is given by

$$S = (1+R)^{-1},\ \ T = R(1+R)^{-1},\ \ J = 1 + R^{-1} \qquad (13)$$

From the small gain theorem [8], the following conditions should be satisfied to guarantee the robust stability.

$$\|\Delta m(s)\| < \|J\|,\ \ \|\Delta a(s)\| < \|S^{-1}\| \qquad (14)$$

This relation is shown in Fig. 6, which describes the singular values of uncertainty models together with the size of J and S^{-1} when the delay is 1.5 sec. The singular values of the uncertainty models shift downward for the shorter delay and the system is robust stable for the delay of up to 1.5 sec. Finally the multiplicative stability margin (MSM) and the additive stability margin (ASM) are found to be

$$\mathrm{MSM} = \left(\sup_{\omega}|T(j\omega)|\right)^{-1} = 1.0021$$
$$\mathrm{ASM} = \left(\sup_{\omega}|S(j\omega)|\right)^{-1} = 0.9228 \qquad (15)$$

These margins of MSM and AMS indicate the minimum size of the uncertainty models which make the system unstable and are more conservative conditions than the conventional gain and phase margins.

3. System Controller on the Level Feedback Loop

There are four inputs which act on the steam generator, that is, feedwater flow rate, steam flow rate, primary coolant temperature and feedwater temperature. The open loop transfer function between each of these inputs and the level is a function of power. In pervious studies [4], [5], the transfer functions were determined by the steady state power at which a transient starts and were assumed to be constant during the transient.

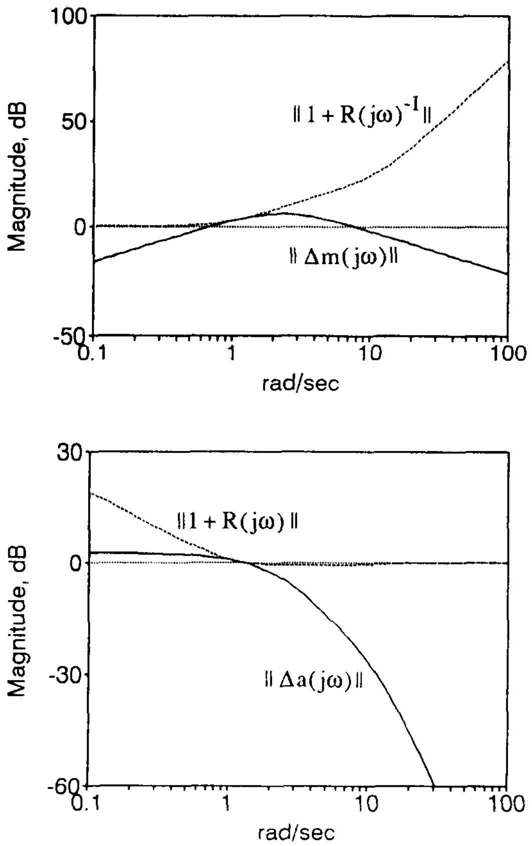

Fig. 6. Margins of Uncertainty Models

The general approach to the control system design is a trade off the conflicting control specifications such as system speed and stability. For example, if a system is unstable, the gain should be decreased to keep the stability. On the other hand, when the system has a sufficient stability, it is desirable to increase the gain to speed up the system. It is the same for the steam generator. The steam generator is unstable at low power, but becomes more stable with the increase of power. Therefore it may be too conservative to keep the same control constants during the power increase because the system shifts into the stable region. On the contrary, the system may become unstable for the case of power decrease since it gets into the unstable region. On account of these facts, a controller whose control constants change continuously to reflect the varying plant characteristics during the transient is considered, and is to be named dynamic controller hereinafter.

The overall dynamic steam generator level and feedwater control system is outlined in Fig. 7. The system is MIMO (multi input multi output). The steam flow rate is input to the system as a command signal and the outputs are power and level. The level signal is feedbacked and summed with the input signal. The feedback loop of the feedwater is embedded in the feedwater station. It is to be noted that the steam flow rate signal goes directly to the steam generator with other disturbance signals of the primary coolant and feedwater temperatures. The power signal changes the characteristics of steam generator, and the controller is to be modulated by the power. This relation is described by dotted lines.

Figure 8 is the same as Fig. 7, but is described in MISO (multi input single output) by using the transfer function blocks which depend on the power. $\triangle U_i(s)$, where $i=2, 3, 4$, indicates the input signal of the steam flow rate, primary coolant temperature and feedwater temperature, respectively, and $H_i(s)$ is the transfer function which corresponds to each input and is a function of power.

It should be understood clearly that the system is a regulating system in that the level should maintain the predetermined value regardless of the input signal changes. And for a regulating system, with the condition of controllability, it is possible to build a LQR controller which compensates off for the disturbance signals to make the input energies to the plant zero. However, since the steam flow rate acts on the plant directly, or physically the steam always comes out from the plant, it has no sense to compensate for the input signal by the LQR feedback signals, and the overall control structure should be such the one as described in Fig. 8 using a PID controller.

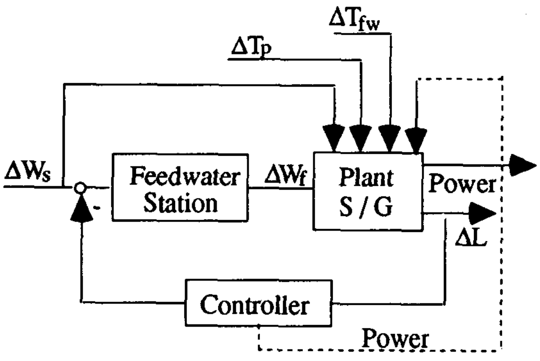

Fig. 7. Power Dependent S/G Level Control System

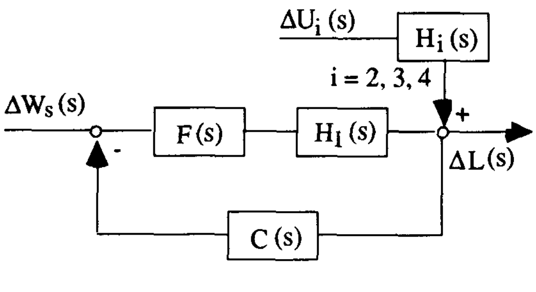

Fig. 8. S/G Level Control System Described by Power Dependent Transfer Functions

From Fig. 8 the feedwater flow rate to the steam generator and the level output are

$$\Delta W_f(s) = \frac{\Delta W_s(s)F(s)\left(1 - C(s)H_2(s)\right) - F(s)O(s)}{1 + F(s)H_1(s)C(s)}$$

$$\Delta L(s) = \frac{\Delta W_s(s)\left(H_2(s) + F(s)H_1(s)\right) + O(s)}{1 + F(s)H_1(s)C(s))}$$

$$O(s) = T_p(s)H_3(s) + T_{fw}(s)H_4(s) \tag{16}$$

The transfer function $H_i(s)$ in the above equations are subject to change continuously with the power, and the power should be determined first to obtain the feedwater flow rate and level. For the numerical calculations, the relationship between each input and the power variation has been derived in the form of transfer function as below.

$$P_i(s) = \frac{\Delta P(s)}{\Delta U_i(s)} \tag{17}$$

where $i=1, 2, 3, 4$ and indicates the feedwater and steam flow rate, primary coolant and feedwater temperature, respectively.

The thermal-hydraulic code developed in Ref. [3] is used to determine the $P_i(s)$. It is found that the power variation itself is a function of power also. For example, Fig. 9 shows the responses of power variation for the unit step increase of the feedwater flow when the initial power is 5%, 10% and 15%, respectively. The solid lines are results of the code calculation and dotted lines are by the Laplacian inversion of $P_i(s)$. As the power becomes lower, the output response gets unstable. In defining $P_i(s)$s, which are summarized in Table 1, typical and simple transfer functions of the first and the second order forms are used. The more exact description is possible with the higher order functions, but they introduce the increase of state order and it takes a long time to simulate.

Figure 10 also shows the step responses of power variation for the feedwater step changes whose magnitudes are 5 and 10 Kg/sec, respectively. The solid lines are for the case of which the power variation is feedbacked to recalculate the $P_i(s)$ (dynamic), and the dotted lines are for the constant $P_i(s)$ which is determined by the initial power (non-dynamic). For the case of dynamic, the speed increases with a small damping. It should also be noted that the output shapes of the dynamic case are not the same each other for the different step magnitudes of the feedwater while the non-dynamic case shows the same

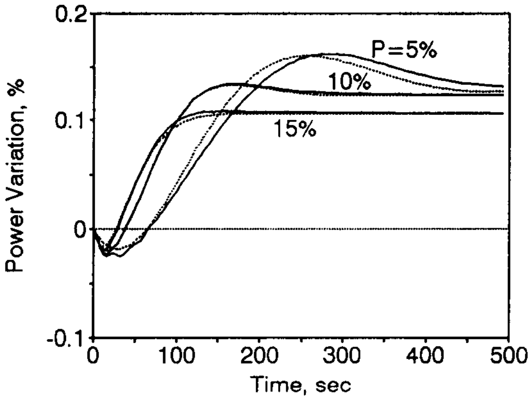

Fig. 9. Power Variation for Unit Step Change of Feedwater Flow Rate

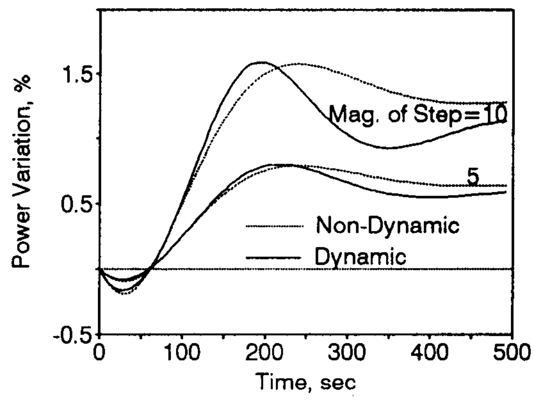

Fig. 10. Power Variation for Different Magnitude Step Changes of Feedwater Flow Rate

Table 1. Transfer Functions Between Various Imputs and Power

1. Feedwater Flow Rate $P_1(s)=K_1\dfrac{as+\omega^2}{s^2+2\varsigma\omega s+\omega^2}$ $K_1=-1.753\cdot10^{-4}p^2+9.483\cdot10^{-4}p+0.1314,\quad p\le20$ $=-3.1803\cdot10^{-6}p^3+3.7698\cdot10^{-4}p^2-1.5106\cdot10^{-2}p+0.2564,\quad p>20$ $a=-0.001p-0.005,\quad p\le5$ $=-0.002\,p,\quad 5<p\le20$ $=-0.04,\quad p>20$ $\varsigma=1.4\cdot10^{-3}p^2+1.5\cdot10^{-2}p+0.36,$ $=0.9,\quad p>15$ $\omega=2.34\cdot10^{-3}p+0.004,\quad p\le20$ $=0.05,\quad p>20$ 2. Steam Flow Rate $P_2(s)=0.185\dfrac{0.05}{s+0.05},\quad p\le15$	$=\dfrac{\omega^2}{s^2+2\varsigma\omega s+\omega^2},\quad p>15$ $\varsigma=-0.0022p^2+0.115p-0.23$ $\omega=4\cdot10^{-4}p+0.04$ 3. Primary Coolant Temperature $P_3(s)=K_3\dfrac{(a-b)s}{(s+a)(a+b)}$ $K_3=2.5,\quad a=0.35,\quad b=a/10,$ for all power 4. Feedwater $P_4(s)=K_4\dfrac{a}{s+a}e^{-ds}$ $K_4=-2.6\cdot10^{-5}p^2-0.00125p-0.0012,\quad p\le15$ $=-0.00256\,p+0.01225,\quad p>15$ $a=1\cdot10^{-4}p+0.0295,$ for all power $d=0.3p^2-8.5p+85,\quad p\le15$ $=-0.4484\,p+30.9,\quad p>15$

responses except the magnitudes. This is because $P_i(s)$ is determined by the initial power and is held constant during the transient for the non-dynamic case.

The controller on the level feedback loop, C(s), is an ordinary PID controller. But the system speed is slow enough to neglect the differentiator, and the controller constants of gain and integration time are determined as [5]

$$C(s) = K\left(\frac{1 + T_I s}{T_I s}\right)$$

$$K = 34.3 + 3.85\,P + 0.2\,P^2 \qquad (18)$$

$$T_I = 641.3 - 60\,P + 2.1\,P^2$$

where P is the initial power. The control constants of above equation were determined under the constraint of that the overall system should have the phase margin of more than 30 degrees for any initial power, and the gain can be increased with the power. However, if the constants are held constant during the power decrease, the system gets unstable. The initially determined gain is too large to maintain the stability since the plant characteristics becomes more unstable as the power decreases. This will be discussed later.

4. Digitalization and Simulation

The feedwater controller and the level feedback controller are designed in the continuous s-domain, and it is necessary to digitalize them for the actual use. The digitalization of the continuous controller already designed is so called an indirect method. This method has an advantage of the simplicity, but since the discretization schemes are always approximations, the resulting digital controller may be different from the original continuous one. The degree of approximation depends on the sampling period which is a key parameter in converting a continuous system to a digital system [9].

The selection of the sampling period, Ts, is made based on the speeds of the plants which comprise the system. It is found that the speeds of $H_i(s)$ and $P_i(s)$ are very slow, which is the general property of the thermal-hydraulic processes [10]. For example, the natural frequency, which is the direct index of the speed, of $H_i(s)$ ranges from about 0.01 to 0.5 rad/sec depending on the power. This means that the system is not so sensitive to the sampling period. For the case of feedwater station, the Bode diagram in w-domain indicates that the bandwidth is 1.07 rad/sec, which is faster than $H_i(s)$ or $P_i(s)$. Therefore, from the Nyquist frequency condition of $Ts < \omega\pi$, the upper bound of Ts is determined as about 3.4 seconds.

In general, it is thought that there is no limitation on the lower bound of Ts, which is not always true. If Ts is too small, the controllability matrix of the discretized system may not satisfy the rank condition and the system properties become different from those of original system [7]. This is described in Fig. 11 which shows the frequency responses of the characteristic function of the overall system, $F(w)H_1(w)C(w)$, in w-domain for different sampling periods of 0.1, 1 and 5 seconds when the initial power is 5%. The frequency response of the original continuous system is also drawn on the same figure for comparison. When the sampling period is 5 seconds, the frequency response deviates from the original one at about 0.6 rad/sec, and the larger the Ts is, the more deviations there are in the high frequency region. On the contrary, the small sampling period of 0.1 second shows a deviation at low frequencies although it conforms to the original one at high frequencies. As mentioned above, the actual operating frequency of the system ranges from 0.01 to 1 rad/sec. Therefore it is plausible to determine the sampling period as 1 second, which is used in all the simulations below.

For the simulations, the system described in Fig. 8 is used. All the continuous plants are discretized by introducing the ZOH (zero order holder) transformation while the controllers are by the Tustin transformation. The calculation procedure is such that the power at a given moment is obtained first from the duplicated scheme of Fig. 8 in which $H_i(s)$s are replaced by $P_i(s)$s and then this power is used to determine the new $H_i(s)$s and $P_i(s)$s for the next time step. The overall system is converted to a set of state equations and the dimension of the system matrix is 19 by 19. The state equations are solved by MATLAB [11] at each time step.

The input conditions are the same as those of Refs. [4] and [5]. That is, for the power increase from 5 to 10%, the steam flow rate is increased linearly at the rate of 0.273 Kg/sec from t=10 to 70 second, and the primary temperature is increased linearly by 0.03°C from t=25 to 70 second and again by 0.026°C from t=70 to 80 second. There is no feedwater temperature change in the power range of 5 to 10%.

Two cases are considered in numerical simulations. One is the case of which that the plants of $H_i(s)$s and $P_i(s)$s are subject to change continuously with the power variation but the control constants of C(s) are fixed to the values which are determined by the initial power. This case is to be named semi-dynamic run in this paper. The other, which is named dynamic run, is the case of which the controller constants, as well as $H_i(s)$s and $P_i(s)$s, change with the power. The terminologies are explained in Table 2 for the purpose of convenience.

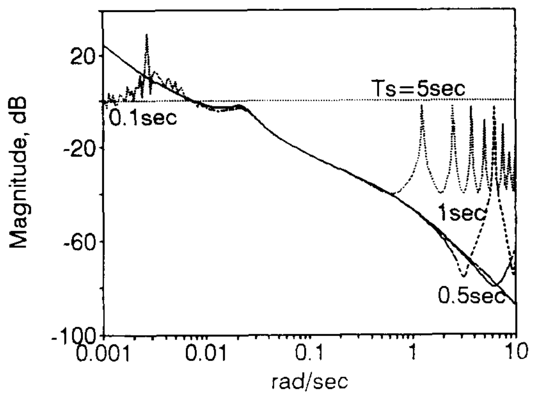

Fig. 11. Frequency Responses of Digital System for Different Sampling Periods

Table 2. Explanations on Simulation

Simulation	Plant	Controller
Dynamic	$H_i(s)$ and $P_i(s)$ are dependent on power	C(s) depends on power (Dynamic Cont.)
Semi-Dynamic	$H_i(s)$ and $P_i(s)$ are dependent on power	C(s) is constant
Non-Dynamic	$H_i(s)$ and $P_i(s)$ are constant	C(s) is constant

Figures 12 (a) through (d) show the variations of the level, feedwater flow rate, power and controller gain for the case of semi-dynamic as well as for the dynamic calculation. Also shown are the results of the previous study [5] in which the plants and controller were assumed to be constant during the transient (non-dynamic). First, it can be found that the peak water levels of both the semi-dynamic and dynamic cases are less than those of non-dynamic case. Those peak values are more realistic since the plants change in a real situation. Particularly, the feedwater variation of the semi-dynamic case shows a milder response. This is due to the LQR feedwater station design in which the input magnitude is considered as a design constraint. The results of dynamic run are not so good as those of semi-dynamic run, although they are stable. This is because the dynamic controller gain which is determined from Eq.(18) by using P(t), instead of the initial power, increases too much with the power.

Considered also is the case of power decrease. The operating input conditions are given as opposite directions of the power increase. The responses of both the semi-dynamic and dynamic cases are described in Figs. 13 (a) through (d). As is expected, the results of the semi-dynamic run show unstable transients. This is because the gain which is determined at high power is too large to keep the same margin of stability since the plant becomes unstable

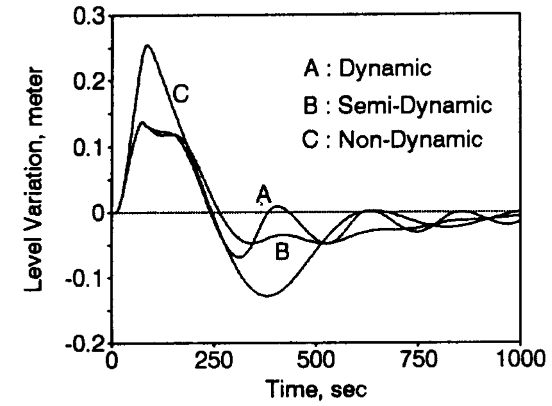

Fig. 12 (a). Transients of Level Variation, 5% to 10% Power Increase

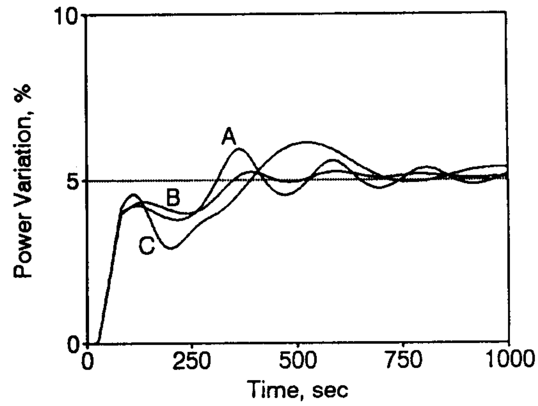

Fig. 12 (c). Transients of Gain Variation, 5% to 10% Power Increase

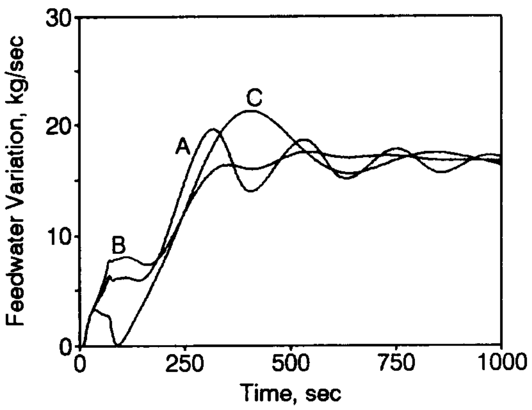

Fig. 12 (b). Transients of Feedwater Variation, 5% to 10% Power Increase

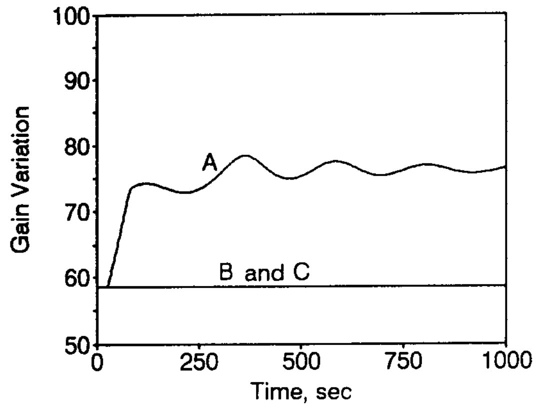

Fig. 12 (d). Transients of Gain Variation, 5% to 10% Power Increase

at low power. In contrast with the semi-dynamic, the dynamic calculation results in better transient characteristics. The minimum water level is less than -0.2 meter and the feedwater variation is not so severe.

From these facts, two modes of controller setting could be proposed. When the power is increased, the controller constants are to be held constant until a new equilibrium state is reached, and for the case of power decrease, the controller should be of a dynamic type whose control constants are changed with the power variation.

5. Conclusions

The steam generator feedwater and level control system is designed by two steps. The controller of the feedwater servo system is determined first and then the controller on the level feedback loop is considered. The feedwater controller design is made by the LQR method to consider the constraints on both the states and the input energy. On account of the uncertainties of the system and measurement noises, an observer is constructed by the LTR approach since the ordinary LQG method does not guarantee the

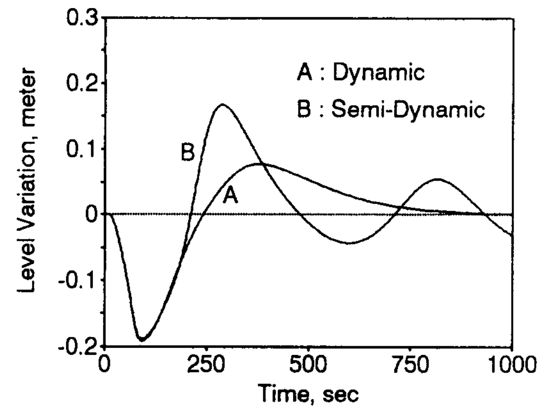

Fig. 13 (a). Transients of Level Variation, 10% to 5% Power Decrease

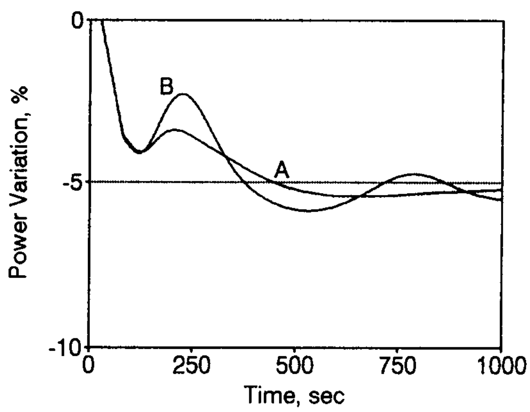

Fig. 13 (c). Transients of Power Variation, 10% to 5% Power Decrease

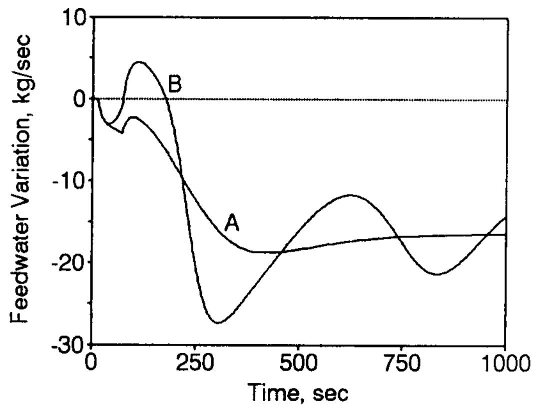

Fig. 13 (b). Transients of Feedwater Variation, 10% to 5% Power Decrease

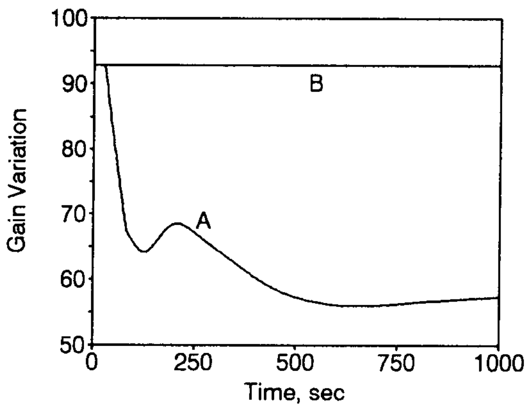

Fig. 13 (d). Transients of Gain Variation, 10% to 5% Power Decrease

system robustness.

The controller designed by this method shows a good robustness in the presence of severe system perturbations. The constants of the controller on the feedback loop is determined to maintain the same stability margin for all power levels.

Since all the transfer functions between the input signals to the steam generator and the level are subject to change with the power variations, the relations between input signals and their corresponding output of power variation are described in the simple form of transfer functions. The power variation is then used to determine the new transfer functions and the values of feedback loop controller constants.

For the digitalization of the controller, the sampling period, which is a key parameter of the digital design, is determined as 1 second by investigating the system speed and frequency responses. Two kinds of simulations are made. The first is the case of which all the properties of plants are varying with power but with the fixed controller, and the second is the case of which the the controller, as well as the plants, changes with power. From the results of simulation, it is found that the constant controller is desirable during the power increase, but the controller constants should be changed with the power variation for the case of power decrease.

Acknowledgement

This paper was supported by Non-Directed Research Fund, Korea Research Foundation.

References

1. L.W. Pearce et al., "How Digital Low Power Feedwater Control Can Minimize Plant Trips," *Nuc. Eng. Int'l.* (1988)
2. "Feedwater System Operability Improvement," Westinghouse WOG 1988 Trip Reduction Conference (1988)
3. Y.J. Lee, "Water Level Control of Nuclear Generator." *Trans. on KSME J.*, **16**, 753−764 (1992)
4. Y.J. Lee, U.C. Lee, "Digitalization of Nuclear S/G Water Level Control System," *J. of KNS*, **25**, 126−135 (1993)
5. Y.J. Lee, "Optimal Design of the Nuclear S/G Digital Water Level Control System," *J. of KNS*, **26**, 32−40 (1994)
6. J.C. Doyle, et al., "Robustness with Observers," *IEEE Trans. Auto. Cont.*, **24**, 607−611 (1979)
7. F.L. Lewis, *Applied Optimal and Estimation*, Prentice Hall (1992)
8. J.M. Maciejowski, *Multivarable Feedback Design*, Addison Wesley (1989)
9. G.F. Franklin et al., *Digital Control of Dynamic Systems*, Addison Wesley (1990)
10. K. Ogata, *Discrete Time Control System*, Prentice Hill (1987)
11. MATLAB, Ver. 4.0, Math Work Inc. (1992)